



# Water sorption in wood cell walls—data exploration of the influential physicochemical characteristics

Maria Fredriksson · Markus Rüggeberg ·  
Thomas Nord-Larsen · Greeley Beck ·  
Emil Engelund Thybring

Received: 19 March 2022 / Accepted: 24 November 2022  
© The Author(s) 2022

**Abstract** The material properties of wood are intimately tied to the amount of moisture contained in the wood cell walls. The moisture content depends on the environmental conditions, i.e. temperature and relative humidity, but also on material characteristics of the wood itself. The exact mechanisms governing moisture equilibrium between wood cell walls and environmental conditions remain obscure, likely because multiple material characteristics have been proposed to be involved. In this study, we used a data exploration approach to illuminate the important wood

characteristics determining the cell wall moisture content in the full moisture range. Specimens of nine different wood species (two softwoods and seven hardwoods) were examined in terms of their material characteristics at multiple scales and their cell wall moisture content was measured in equilibrium with both hygroscopic conditions and at water-saturation. By statistical analysis, the chemical composition was found to be the most important predictor of the cell wall moisture content in the full moisture range. For the other wood characteristics the importance differed between the low moisture range and the humid and saturated conditions. In the low moisture range, the cellulose crystallinity and hydroxyl accessibility

**Supplementary Information** The online version contains supplementary material available at <https://doi.org/10.1007/s10570-022-04973-0>.

M. Fredriksson (✉)  
Division of Building Materials, Department of Building and Environmental Technology, Lund University, Lund, Sweden  
e-mail: maria.fredriksson@byggtek.lth.se

M. Rüggeberg  
Institute for Building Materials, Swiss Federal Institute of Technology Zürich (ETH Zürich), Zurich, Switzerland

M. Rüggeberg  
Laboratory of Cellulose and Wood Materials, Swiss Federal Laboratories for Materials Science and Technology (Empa), Dübendorf, Switzerland

*Present Address:*  
M. Rüggeberg  
Institute for Forest Utilization and Forest Technology, Technische Universität Dresden, Dresden, Germany

T. Nord-Larsen  
Forest Resource Assessment and Bioenergy, Department of Geosciences and Natural Resource Management, University of Copenhagen, Frederiksberg, Denmark

G. Beck  
Department of Wood Technology, Norwegian Institute of Bioeconomy Research, Ås, Norway

*Present Address:*  
G. Beck  
Dynea AS, Lillestrøm, Norway

E. E. Thybring (✉)  
Bioresource Chemistry and Technology, Department of Geosciences and Natural Resource Management, University of Copenhagen, Frederiksberg, Denmark  
e-mail: eet@ign.ku.dk

were found to be important predictors, while at high moisture contents the microfibril orientation in the S1 and S3 layers of the cell walls was important. Overall, the results highlighted that no single wood characteristic were decisive for the cell wall moisture content, and each of the predictors identified by the analysis had only a small effect in themselves on the cell wall moisture content. Wood characteristics with a major effect on the cell wall moisture content were, therefore, not identified.

**Keywords** Moisture · Moisture content · Sorption · Sorption isotherm · Wood

## Introduction

The physical properties of wood are profoundly affected by water within the material, often referred to as moisture. Wood-water relations are central to the utilisation of wood in society as they affect everything from mechanical performance to fungal decay of the material. Therefore, a myriad of studies within wood science has been devoted to understanding the fundamental mechanisms of how wood and moisture interact (Thybring et al. 2022; Engelund et al. 2013; Skaar 1984; Venkateswaran 1970).

Wood is a porous material that can take up water in both its cell walls and macro-void structure. For the latter, water is taken up either by capillary condensation of water vapour or by capillary action when in contact with to liquid water. For wood without direct contact with liquid water, capillary condensation is the fundamental mechanism governing moisture uptake (sorption) from water vapour (Fredriksson 2019), however, it only makes a significant contribution at extremely high air humidity (>99% relative humidity) because of the large size of the macro-voids (Engelund et al. 2010; Thygesen et al. 2010; Fredriksson 2019; Fredriksson and Thybring 2019). Below this humidity range, moisture sorption is dominated by water molecules absorbed within the solid cell walls (Thygesen et al. 2010; Fredriksson and Thybring 2019). Here they interfere with internal hydrogen bonds between wood polymers (Chow 1972; Taniguchi et al. 1978) which dramatically changes the physical wood properties. Despite substantial progress in our

understanding of wood-water interactions in the last decade, as highlighted in recent reviews of the topic (Arzola-Villegas et al. 2019; Chen et al. 2019; Fredriksson 2019; Jakes et al. 2019; Nopens et al. 2019; Plaza 2019; Ringman et al. 2019; Thybring et al. 2019), there is still no consensus about what governs moisture sorption in the cell walls. Various contributing factors have been suggested in literature or can be envisioned, spanning from the nano-scale to the tissue-scale.

On the nano-scale, the number of hydroxyl groups accessible for binding water molecules has been an often stated explanation of the hygroscopicity of wood (Rautkari et al. 2013). However, the role of hydroxyl accessibility in controlling the cell wall moisture content has also been questioned, mainly based on studies on modified wood (Hill et al. 2021; Rautkari et al. 2013; Thybring et al. 2020b). The major chemical components of the cell walls, i.e. cellulose, hemicelluloses, and lignin, differ in concentration of hydroxyls with cellulose having the highest concentration followed by the hemicelluloses (Engelund et al. 2013). However, not all hydroxyls of wood are available to interact with water, since many of them are locked up inside the cellulose microfibrils (Hofstetter et al. 2006; Salmén and Bergström 2009). The microfibrillar surface-to-volume ratio is accordingly linked with their amount of accessible hydroxyls (O'Sullivan 1997). Since cellulose chains on microfibrillar surfaces have a less ordered bonding pattern than those in the core, the previous are often referred to as amorphous (Atalla et al. 2009). The crystallinity of the cellulose could therefore serve as a proxy for the surface-to-volume ratio of microfibrils (Verlhac et al. 1990), and hence as a proxy of the cellulose hydroxyl accessibility (Howsmon 1949; Lang and Mason 1960; Loelovitch and Gordeev 1994; Mann and Marrinan 1956; Pennings et al. 1961). Alternatively, moisture uptake in cell walls could rather be controlled by the chemical composition of the cell walls through inherent differences in the hygroscopicity (moisture attraction) of the individual cell wall polymers (Christensen and Kelsey 1958; Christensen and Kelsey 1959).

One factor on the nano-scale that is known to affect moisture sorption is the amount of extractives in cell walls (Ahlgren et al. 1972; Nzokou and Kamdem 2004; Vahtikari et al. 2017; Wangaard and Granados 1967; Zhou et al. 2016). Extractives vary

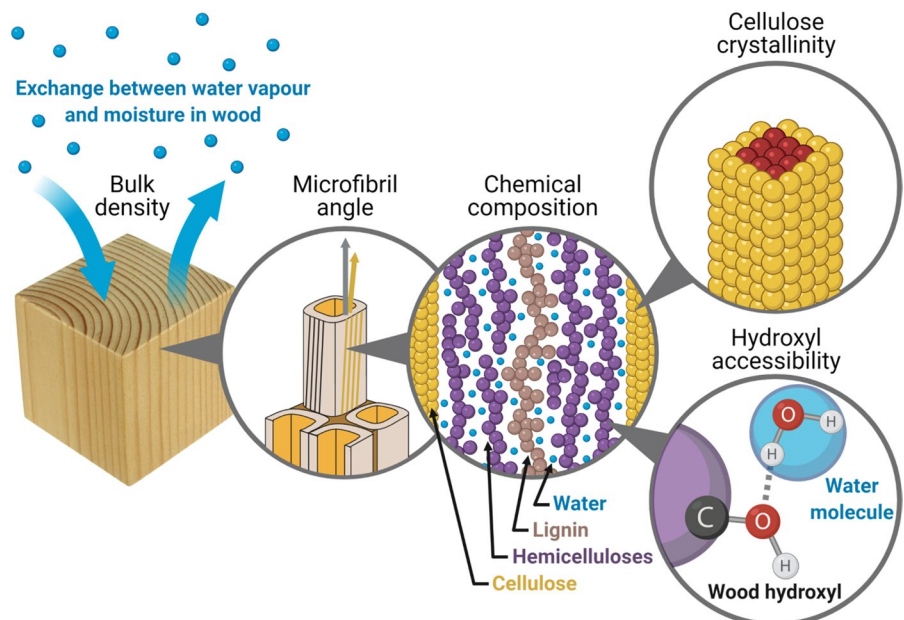
considerably in their chemistry and concentration across wood species, but they are mainly found encrusting heartwood, i.e. the wood in the inner core of the tree, with only smaller amounts being present in the sapwood (Nzokou and Kamdem 2004; Vahtikari et al. 2017; Wangaard and Granados 1967; Zhou et al. 2016). Presence of extractives generally lower the equilibrium moisture content (Füchtner et al. 2020; Nzokou and Kamden 2004; Vahtikari et al. 2017; Wangaard and Granados 1967).

A very noticeable effect of moisture sorption in wood is the accompanying dimensional changes, i.e. shrinkage and swelling. If swelling and shrinkage are restrained, this should, thus, affect the moisture sorption. Swelling and shrinkage can be found on all levels of organisation (Murata and Masuda 2006; Noack et al. 1973; Rafsanjani et al. 2014; Zabler et al. 2010). However, an important factor limiting this behaviour on the micro-scale is the orientation of the long, stiff cellulose microfibrils that reinforce the cell walls (Balashov et al. 1957; Harris and Meylan 1965; Meylan 1972; Zabler et al. 2010). Another factor that could be limiting dimensional changes is the bulk density of the wood (Feist and Tarkow 1967; Gao et al. 2015; Vorreiter 1963). Thus, the thick cell walls in high-density wood species walls have been suggested to have limited capacity for shrinkage/swelling to accommodate

water, whereas the more mechanically compliant walls of thin-walled, low-density wood do not limit dimensional changes as much (Feist and Tarkow 1967). On the other hand, density has been found to positively correlate with bulk swelling of wood (Derome et al. 2011; Newlin and Wilson 1919; Yamashita et al. 2009). Additionally, it has been suggested that the higher density and stiffness of latewood in softwood species affects the swelling of the earlywood (Patera et al. 2013; Patera et al. 2018).

Many studies in literature have tried to correlate moisture sorption with physical wood characteristics of a particular wood species. In this study, we used a different approach to explore which intrinsic wood characteristics influence the cell wall moisture content. We acquired experimental data on a range of physical and chemical characteristics for the wood of nine wood species, see Fig. 1. At the same time, we determined the cell wall moisture content under different climates, both in the hygroscopic moisture range and in water saturated state. By statistically guided data exploration, we zoomed in on the important wood characteristics that correlated with the cell wall moisture content at a given climate. Since it has already been established that extractives affect moisture sorption, this study focused on the influence of other material

**Fig. 1** Schematic overview of investigated characteristics from the tissue-scale (left) to the nano-scale (right). The microfibril structure illustrated under “Cellulose crystallinity” is based on (Fernandes et al. 2011)



characteristics and extracted materials were therefore used.

## Materials and methods

### Specimen preparation

Wood from nine tree species was included in this study. This collection of materials was the same as was used by Thybring et al. (2020a). Oak (*Quercus robur* L.), beech (*Fagus sylvatica* L.), and ash originated from Switzerland, while the Norway spruce (*Picea abies* (L.) Karst.) and hybrid poplar (*Populus x canadensis* Moench.) materials were from Southern Sweden. Abachi (*Triplochiton scleroxylon* K. Schum.), balsa (*Ochroma lagopus* Sw.), Douglas fir (*Pseudotsuga menziesii* (Mirb.) Franco), and ironwood (*Lophira alata* Banks ex. Gartn.) materials were of unknown origin. All wood materials were cut into cubes with a side length of about 10 mm and the extractives were removed by extraction using a Soxhlet apparatus; first with ethanol and toluene (ratio 1:2) for 24 h and subsequently with acetone and MilliQ water (ratio 9:1) for 24 h.

### Characterisation of wood density

The density of the wood materials was determined before and after Soxhlet extraction for four cubes (side length 10 mm) of each wood species. For these cubes, dry mass and dimensions were measured after drying in a vacuum oven at 60 °C for 48–72 h. Masses were determined with a balance of 0.1 mg

resolution and dimensions were measured with a calliper of 0.01 mm resolution. The dimensions were determined twice in each direction and the average value was used to calculate the volume. The dry density was found by dividing the dry masses with the dry volumes (Table 1). The experimental data for density have also been reported by Thybring et al. (2020a).

### Characterisation of microfibril angle

The microfibril angle (MFA) of all wood species was determined by wide-angle X-ray diffraction (WAXD) with a Nanostar (Bruker AXS, Germany). Cu K $\alpha$  radiation with a wavelength of 1.54 Å was employed. The X-ray beam diameter was about 300  $\mu$ m and the sample-detector distance was set to 90.9 mm. For each species, three to five samples of 4  $\times$  1  $\times$  0.5 mm were glued on a sample holder. For each sample, one diffraction image was taken with a measurement time of 30 min. For cellulose orientation analysis, azimuthal intensity profiles of the (200)-Bragg peak of cellulose were generated from the diffraction images by radial integration with the contribution of amorphous parts being removed by baseline subtraction. These profiles were then fitted with simulated azimuthal intensity profiles, which were generated by a combination of two Gaussian distribution of microfibrils considering the cell geometry of the wood fibre cells according to (Rüggeberg et al. 2013). The fitted azimuthal profiles were then used to determine microfibril angles.

**Table 1** Wood species used in this study along with their measured density before and after extraction. Species are listed after ascending density. Standard deviations are given in brackets. Density data after extraction is not available for balsa since the specimens were deformed during the extraction procedure and it was thus not possible to determine the volume

Wood species	Botanical name	Density (kg m <sup>-3</sup> )	
		Before extraction	After extraction
Balsa	<i>Ochroma lagopus</i> Sw.	90 (9)	-
Abachi	<i>Triplochiton scleroxylon</i> K. Schum.	278 (24)	279 (32)
Poplar	<i>Populus x canadensis</i> Moench.	404 (13)	399 (17)
Norway spruce	<i>Picea abies</i> (L.) Karst.	405 (16)	387 (17)
Douglas fir	<i>Pseudotsuga menziesii</i> (Mirb.) Franco	577 (22)	539 (22)
Beech	<i>Fagus sylvatica</i> L.	606 (9)	572 (5)
Ash	<i>Fraxinus excelsior</i> L.	662 (9)	613 (4)
Oak	<i>Quercus robur</i> L.	751 (13)	695 (9)
Red ironwood	<i>Lophira alata</i> Banks ex. Gartn.	1026 (13)	977 (9)

### Characterisation of chemical composition

The chemical composition of the wood materials was determined by combined Thermogravimetric/Differential scanning calorimetry/Fourier transform infrared (TG/DSC/FTIR) analysis using a Netzsch STA 449F1 (Selb, Germany) combined with a Bruker Tensor FTIR (Billerica, MA, USA) (Dworzanski et al. 1991; Grønli et al. 2002; Yang et al. 2007). Sample material (app. 8 mg) of each wood species was pyrolysed by heating from 42 to 710 °C at a rate of 10 °C min<sup>-1</sup>. Based on analysis of both the mass loss in various temperature ranges and the obtained infrared spectra, the chemical content of cellulose, hemicelluloses, lignin, ash, and residual extractives was determined. The experimental data for chemical composition have also been reported by Thybring et al. (2020a), where more detailed information about the experimental procedure can be found.

### Characterisation of hydroxyl accessibility

The hydroxyl accessibility was determined gravimetrically by deuteration in an automated sorption balance (Pönni et al. 2014; Thybring et al. 2020b; Thybring et al. 2017). A sample was prepared by cutting thin slices from a wood specimen using a razor blade. The sample was then placed in the sample pan in a sorption balance (DVS Advantage, Surface Measurement Systems Ltd., London) and was dried for 6 h at 60 °C (0% RH) using the pre-heater followed by 1 h at 25 °C for thermal stabilisation before the dry mass was measured. To increase the temperature, a ramp from 25 to 60 °C over 10 min was used. Similarly, a ramp was used when the temperature was decreased from 60 to 25 °C. The sample was then conditioned for 10 h at 95% RH/25 °C in deuterium oxide vapour. Finally, the sample was dried a second time at 60 °C followed by 1 h at 25 °C for thermal stabilisation using the same procedure as described above. The hydroxyl accessibility  $c_{\text{acc}}$  (mol g<sup>-1</sup>) was evaluated from the dry masses before and after deuteration as:

$$c_{\text{acc}} = \frac{\Delta m_{\text{dry}}}{m_0(M_{\text{D}} - M_{\text{H}})} \quad (1)$$

where  $\Delta m_{\text{dry}}$  (g) is the difference in dry mass before and after deuteration,  $m_0$  (g) is the initial dry mass,

and  $M_{\text{D}}$  (g mol<sup>-1</sup>) and  $M_{\text{H}}$  are the molar masses of deuterium and normal hydrogen, respectively.

Note that the hydroxyl accessibility determined by deuteration is not the true water accessibility of hydroxyls in the wood, since one-third of the surface hydroxyls on cellulose microfibrils cannot be deuterated from interaction with deuterium oxide (Lindh et al. 2016). This corresponds with about 1.3 mmol per gram cellulose that cannot be deuterated (Thybring et al. 2017). However, based on the chemical composition for each wood species, i.e. the cellulose content, the underestimation of the hydroxyl accessibility can be determined.

### Characterisation of cellulose crystallinity

For the structural analysis of cellulose, wood of all species was cut into small granules, placed on a flat rotating sample holder and then measured in reflection by powder XRD (BRUKER D8 Advance) using Bragg-Brentano geometry ( $\theta$ - $\theta$  geometry). A Cu K $\alpha$  radiation source was used with a wavelength of 1.5406 Å at 40 mA (40 kV) in locked coupled mode. The individual scans were taken in the  $2\theta$  range 5–60°. Cellulose crystallinity index was determined by a multiple peak fit using seven Gaussian peaks (numbered P0–P6) within the  $2\theta$  range 12.5–60°. P0: (1–10) Bragg peak, P1: (110) Bragg peak, P2: contribution of amorphous parts of the cell wall (cellulose, hemicelluloses, and lignin), P3: (200) Bragg peak, P4–6: higher order Bragg peaks. Hereby the following constraints were defined. The position of the peaks was kept in reasonable range of the typical  $2\theta$  angles of the cellulose Bragg peaks including peak 2 for amorphous contribution. The width and height of the (1–10) and (110) peaks was set equal and the width of the (200) peak was set equal to that of the (1–10) and (110) peaks. Table S9 lists all relevant parameters and boundary conditions of the fitted peaks. The cellulose crystallinity was calculated as:  $1 - (A(P2)/\Sigma A(P0-6))$  with A being the area underneath the relevant peak(s). The crystallite size was determined by the Scherrer-equation using the FWHM of the (200) Bragg peak of the same fit.

### Characterisation of cell wall moisture content

Two methods were used to determine cell wall moisture contents; an automated sorption balance



(Williams 1995) was used at and below 95% relative humidity (RH), and Differential scanning calorimetry (DSC) (Fredriksson and Thybring 2019; Simpson and Barton 1991; Zelinka et al. 2012) was used in water saturated state. For the sorption balance measurements, specimens (5 mm x 5 mm x 10 mm) of the nine wood species were vacuum saturated using the following procedure: the specimens were kept in vacuum (0.05 mbar) for 1 h, deionized water was then added while running the vacuum pump. The vacuum pump was then switched off but the specimens were kept under vacuum in water for an additional hour before atmospheric pressure was re-established. A sample for the sorption balance measurement was then prepared by cutting small, thin pieces from a vacuum saturated specimen using a razor blade. Each piece was wiped on a moist cloth before placing it in the sample pan to avoid excess water on surfaces and in the pan but without drying the sample itself. Since wood with a wide range of densities was included, it was not possible to have the same sample mass for all wood species. Also, since the measurements started with water saturated samples it was difficult to cut samples in water saturated state, which ended up at the same dry mass. For these two reasons, the dry mass of an individual sample ranged between 2 mg and 16 mg. After cutting, the sample was placed in the sample pan in an automated sorption balance (DVS Advantage, Surface Measurement Systems Ltd., London) and the desorption isotherm was determined by equilibrating the sample at 20 °C at the following relative humidity (RH) levels: 95, 80, 65, 50, 35, 20 and 0%. Due to the uncertainties with using an equilibrium criterion based on mass change over time (Glass et al. 2018; Glass et al. 2017), fixed equilibration times were used instead. These times were: 60 h at 95% RH, 24 h at 80% RH, 48 h at 0% RH, and 12 h at all other RH levels. Two replicates were used for each wood species, and a total of 18 samples were thus measured. After each measurement, the equilibrium moisture content at each RH level was evaluated as mass of water divided by the dry mass (i.e. the mass at the last step at 0% RH/20°C). In addition, the closeness to equilibrium at each step was evaluated from the rate of sorption, i.e. the change in moisture content over time, found by linear regression in a two hour time window at each RH level (Fig. S2-S3). Based on data by Glass et al. (2018), the change in mass over time was

small enough not to introduce excessive errors in the evaluated moisture contents. Any differences in moisture contents seen between samples should, thus, not be caused by lack of equilibrium.

In the water-saturated state, the cell wall moisture content was determined using DSC by measuring the heat required to thaw a water-saturated specimen quenched to -20 °C. The energy required for thawing relates to the amount of water outside of cell walls (Fredriksson and Thybring 2019; Thybring et al. 2020a). By drying the specimen after the measurement, the dry mass was found and subsequently the total amount of water. From this, the water outside cell walls was deducted and the cell wall moisture content was determined as the difference between the total moisture content and moisture content corresponding to water outside of cell walls; see (Thybring et al. 2020a) for further details. This cell wall moisture content data for the nine wood species as well as the experimental protocol for the DSC measurements have previously been reported by Thybring et al. (2020a).

#### Statistical analysis

Absolute variability (standard deviation) and relative variability (coefficient of variation, CoV) were determined in order to get an overview of the spread in wood characteristics between wood species.

The data was further analysed with least squares general linear models (procedure GLM in SAS, v. 9.4) to determine the statistically significant variables and their contribution to the cell wall moisture.

$$y = \mathbf{x}_s \boldsymbol{\beta}_s + \mathbf{X} \boldsymbol{\beta} + \epsilon \quad (1)$$

where  $y$  is the cell wall moisture content,  $\mathbf{x}_s \boldsymbol{\beta}_s$  is a vector defining the effect of each sub-condition (level of relative humidity),  $\mathbf{X}$  is the design matrix,  $\boldsymbol{\beta}$  is a vector of fixed effects, and  $\epsilon$  is the random error. The first term of the right-hand side describes the variation in moisture content with relative humidity. For this analysis, the moisture content was normalised with the relative humidity used in the conditioning of the samples, to accentuate material properties rather than the conditioning environment. Hence, all results express the wood moisture content relative to the relative humidity of the surrounding environment. Owing to the large number of variables

**Table 2** Variables included in the analyses. Relative humidity was included as a class variable (sub-condition) with seven levels

Variable	Unit	Levels
Hydroxyl accessibility	(mmol g <sup>-1</sup> )	
Cellulose	%	
Hemicellulose	%	
Lignin	%	
Bulk density	g cm <sup>-3</sup>	
Crystallinity index	%	
Microfibril angle (S2 layer)	°	
Microfibril angle (S1 and S3 layers)	°	
Relative humidity	%	20, 35, 50, 65, 80, 95, 100

analysed (Table 2) and the limited number of samples, we analysed only for main effects excluding any interactions between variables analysed. Ash content and residual extractives were a priori left out of the analyses to avoid excess correlation between variables included, i.e. owing to the obvious correlations between the relative content of the wood constituents. We initially analysed the full model including all variables and subsequently reduced the model using backward elimination until all remaining variables were significant ( $P < 0.05$ ). Results were analysed using the Sum of Squares (SS) Type III statistics. Analyses were conducted both for all levels of relative humidity of the conditioning environment as well as specific levels of relative humidity. Thus, the dataset for cell wall moisture content contained between 88 and 196 data points depending on the range of relative humidity investigated.

## Results and discussion

### Variability of wood characteristics

The physical and chemical characteristics of the nine wood species are plotted in Fig. 2. The variability between wood species is given in Table 3 by the absolute variability (standard deviation) and relative variability (coefficient of variation, CoV). Bulk density and content of ash and extractives were the characteristics with the highest coefficient of variation

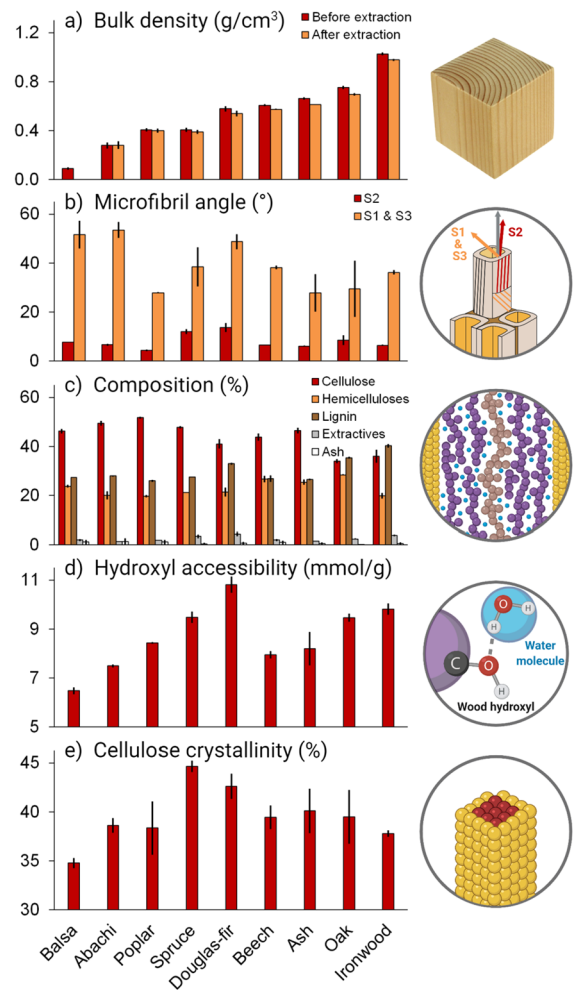


**Fig. 2** Overview of the wood characteristics of the investigated species: **a** bulk density, **b** microfibril angle of the dominant (S2) cell wall layer and the other (predominantly, S1 and S3) layers, **c** chemical composition, **d** hydroxyl accessibility, and **e** cellulose crystallinity index. Values for all characteristics relate to the wood after extraction, except for bulk density with values for both before and after extraction. Error bars mark the standard deviation

in this study. However, for the latter two the standard deviation was of the order of the measurement uncertainty for those characteristics. The CoV of the microfibril angle in the various cell wall layers for all wood species was less than for the bulk density, but they were still among the characteristics with reasonably high variability. The CoV of the chemical composition of the three dominant cell wall polymers and in hydroxyl accessibility were around the same level, while the cellulose crystallinity had the smallest

**Table 3** Compilation of all physical and chemical characteristics of the nine wood species. Average value and standard deviation for each characteristic are based on the

mean values determined for each of the nine wood species. The coefficient of variation was determined from the ratio of standard deviation to the average value

Wood characteristic		Average value	Standard deviation	Coefficient of variation (%)
Bulk density	Before extraction ( $\text{g cm}^{-3}$ )	0.5	0.3	48.8
	After extraction ( $\text{g cm}^{-3}$ )	0.5	0.3	52.4
Microfibril angle	S2 ( $^{\circ}$ )	7.9	2.8	35.7
	S1 & S3 ( $^{\circ}$ )	39.1	9.5	24.3
Composition	Cellulose (%)	44.0	5.7	12.9
	Hemicelluloses (%)	22.9	3.1	13.5
	Lignin (%)	30.0	4.7	15.7
	Ash (%)	0.7	0.4	57.0
	Extractives (%)	2.4	1.0	41.2
Hydroxyl accessibility (mmol/g)		8.7	1.3	14.5
Cellulose crystallinity (%)		39.5	2.7	6.7

variability between the wood species studied. For the hydroxyl accessibility, the underestimation by the deuteration method was estimated to  $0.6 \text{ mmol g}^{-1}$  on average, which gave an average estimated true hydroxyl accessibility for all wood species of  $9.2 \text{ mmol g}^{-1}$  (standard deviation:  $1.2 \text{ mmol g}^{-1}$ ) corresponding with a CoV of 13.2% instead of 14.5% (Table 3). Thus, the slight underestimation by deuteration only shifts the determined hydroxyl accessibility to lower levels, but does not change the variability.

#### Cell wall moisture content

The moisture content data for the nine wood species under hygroscopic and water-saturated conditions show that the moisture content varied more between all wood specimens as the relative humidity increased (Figs. 3 and 4). This is expected if there is a systematic difference in the hygroscopicity between the wood species. However, the coefficient of variation (CoV) in Table 4 decreased slightly between 20% and 80% RH, but was small in relation to the CoV at 95% RH and in water saturated state (Table 4). This indicates that the relative differences in moisture content between wood species were nearly constant between 20% and 80% RH, but increased at 95% RH and in water saturated state. Similar results were found by Choong and Manwiller (1976) who investigated 22 hardwood species and found a nearly constant CoV of 2.8–3.4% below 70% RH, but an increasing CoV

above. Additionally, the results of Ahmet et al. (2000) for six softwood species and 12 hardwood species showed a constant CoV of about 7% between 35 and 75% RH at 10, 20, and 30 °C.

It is not evident why the difference in moisture content between all wood specimens was larger in both absolute and relative terms at 95% and 100% RH (Table 4; Fig. 3). One possibility is that this is related to the presence of capillary condensed water in the macro-void structure in some of the wood species although this is typically reported to affect the moisture content insignificantly in the hygroscopic range, even at 95% RH (Fredriksson and Thybring 2019; Hoffmeyer et al. 2011). However, a few studies have observed liquid water in the range 86–90% RH in desorption for sugar maple (*Acer saccharum* Marsh.) (Hernández and Cáceres 2010), *Eucalyptus saligna* (Passarini et al. 2015), and red oak (*Quercus rubra* L.) (Passarini et al. 2015) using Magnetic resonance imaging (MRI). The capillary water found in these studies was associated with libriform fibers, parenchyma cells, and intercellular spaces where water was held in desorption because of small openings that hindered emptying. Based on these studies, one could therefore argue that the differences seen at 95% RH potentially could be caused by the presence of capillary water in a few of the wood species such as ash, oak, and beech that all had higher moisture content than the average (Fig. 3). This does, however, not explain the differences seen at 100%



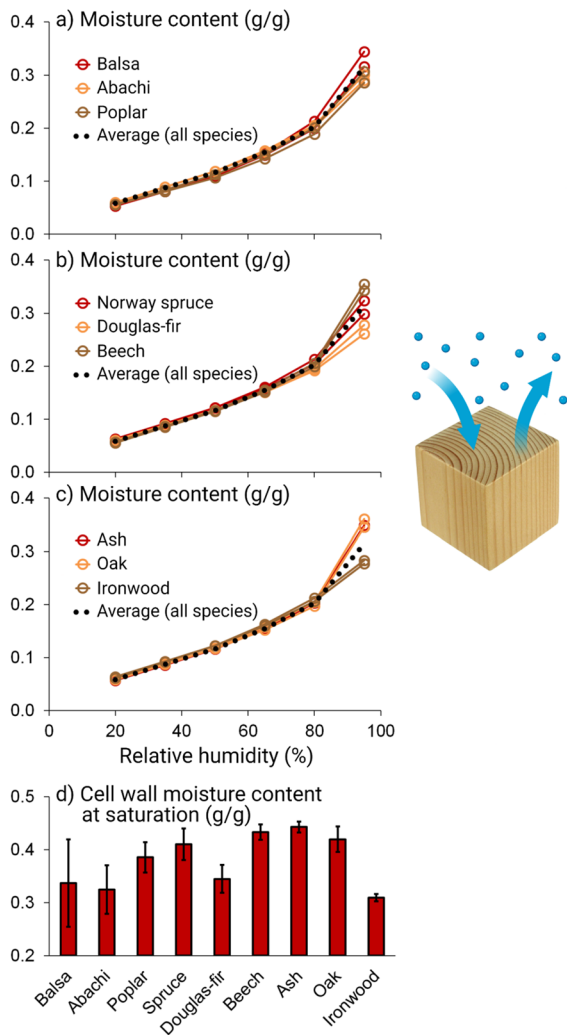


**Fig. 3** a–c Moisture contents in the hygroscopic range (20–95% RH) for the nine wood species with average curve for all species, and **d** cell wall moisture content in the water-saturated state (error bars indicate standard deviation) for the nine wood species

RH (water saturated state), where the evaluated cell wall moisture content is presumed to only contain cell wall water since it was determined by DSC and the capillary water changes phase in the temperature range  $-20$  to  $+20$  °C. Although non-freezing capillary water (adsorbed water on surfaces within the macro voids) might exist, these amounts have previously been reported to be insignificant (Thybring et al. 2020a) and should, thus, not affect the evaluated moisture content. Figure 3d shows that ash, oak, and beech had cell wall moisture

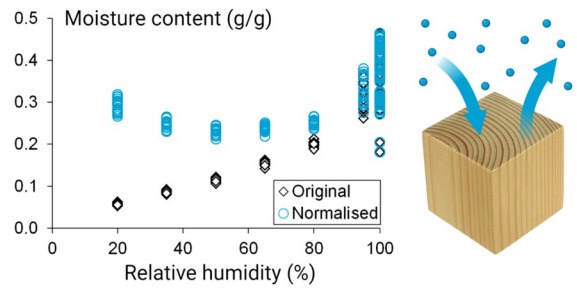


**Fig. 4** Data for the cell wall moisture content of all wood species as function of relative humidity along with the same data normalised by the water activity, i.e. the fractional relative humidity of the air

**Table 4** Compilation of all moisture content data for the nine wood species. The coefficient of variation was determined from the ratio of standard deviation to the average value

Relative humidity (%)	Average value ( $\text{g g}^{-1}$ )	Standard deviation ( $\text{g g}^{-1}$ )	Coefficient of variation (%)
20	0.059	0.003	5.1
35	0.087	0.004	4.3
50	0.117	0.004	3.8
65	0.154	0.005	3.1
80	0.203	0.007	3.2
95	0.315	0.031	9.8
100	0.379	0.060	15.9

content higher than the average, also in the water saturated state. Therefore, since differences between wood species were observed both at 95% and at 100% RH using different methods, and presence of capillary water could only be a possible explanation in one case, it is unlikely that the difference in cell wall moisture content between wood species was a result of presence of significant amounts of capillary water in some of the species. Instead in the following sections, we will discuss, if these differences could be explained by differences in any of the determined wood characteristics.

#### Correlations between wood characteristics and moisture content

The chemical composition was the most important predictor of the cell wall moisture content at both high humidity levels (95–100% RH) and for

**Table 5** Physical and chemical characteristics affecting the cell wall moisture content at different climates and the  $P$ -values for those that were statistically significant ( $P \leq 0.05$ ). Effects of RH level on the cell wall moisture content are not

shown. Further details about the results of the statistical analysis and partial  $R^2$ -values are found in the Supplementary Material

Wood characteristic		Relative humidity range (%)				
		20–100	20–80	80–100	95–100	100
Bulk density		n.s.	0.0341	n.s.	n.s.	n.s.
Microfibril angle	S2	n.s.	n.s.	n.s.	n.s.	n.s.
	S1 & S3	<0.0001	n.s.	<0.0001	<0.0001	<0.0001
Composition	Cellulose	<0.0001	<0.0001	<0.0001	<0.0001	<0.0001
	Hemicelluloses	n.s.	n.s.	n.s.	n.s.	n.s.
	Lignin	0.0055	<0.0001	<0.0001	<0.0001	<0.0001
Hydroxyl accessibility		0.0202	<0.0001	0.0453	0.0465	n.s.
Cellulose crystallinity		0.0039	<0.0001	0.0204	0.0161	0.0418
$R^2$ -value for total model		0.825	0.936	0.790	0.733	0.709

different levels of hygroscopic conditions (20–80% RH) (Table 5). The three dominant components of the chemical composition were naturally not independent as they all sum up to nearly 100% with the combined content of ash and extractives found in the range 1.8–4.8%. It is, therefore, not necessarily of significance which of the cell wall components correlates well with the cell wall moisture content, but the analysis singled out the contents of cellulose and lignin as significant characteristics in relation to the cell wall moisture content (Table 5). Both were negatively correlated with the cell wall moisture content when considering the full moisture range and the range above 80% RH only. Yet slightly positive correlation was observed at 20–80% RH (Table S7). Thus, in general, higher contents of cellulose and lignin, and a lower content of hemicelluloses, were associated with lower cell wall moisture contents, but only for the highest humidity levels included in the evaluation. This is in line with literature, since ex-situ hemicelluloses have been seen to absorb more moisture than ex-situ lignin or cellulose (Christensen and Kelsey 1959). Thus, removal of hemicelluloses have been shown to reduce the cell wall moisture content at water saturation (Elder and Houtman 2013; Yang et al. 2020) and lignin removal increases the moisture content (Yang et al. 2018). It is not clear why the correlation changed sign for the 20–80% RH range compared with the high humidity range. The importance of cellulose and lignin in explaining the variation in cell wall moisture content was,

however, markedly lower at 20–80% RH than at high humidity. This was observed in the partial  $R^2$ -values for these characteristics, which were dominant at high humidity, but were much lower and on level with the hydroxyl accessibility and cellulose crystallinity at 20–80% RH (Table S8).

Another important predictor overall and in particular at high humidity was the secondary microfibril angle (Table 5), i.e. the one dominated by the S1 and S3 layers, which was negatively correlated with the cell wall moisture content. That is, a low microfibril angle in the S1 and S3 layers was associated with a high cell wall moisture content. It is not evident why a significant effect was seen for the orientation of the cellulose microfibrils in the S1 and S3 layers but not for the microfibrils in the much thicker S2 layer. However, this may arise from the stiffening effect of the microfibrils in the S1 and S3 layers in the transverse direction of the cell wall. Thus, variation in the orientation of microfibrils in the S1 and S3 layers affects the transverse stiffness of the cell walls, whereas variation in the orientation in the S2 layer only has a significant effect at high microfibril angles (Bergander and Salmén 2000; Bergander and Salmén 2002; Wang et al. 2013). Since the dimensional changes of the wood cell walls, i.e. shrinkage and swelling, occur predominantly in the transverse directions (Keylwerth 1962), this might explain, why the microfibril angle in the S1 and S3 layers influenced the cell wall moisture content more than changes in the rather small microfibril

angle of the S2 layer, i.e. where the microfibrils are nearly aligned in the longitudinal direction. A lower transverse stiffness that follows from a low microfibril angle in the S1 and S3 layers would decrease the mechanical work of swelling. This in turn could increase the cell wall moisture content in equilibrium with the surrounding environment, which has for instance been observed in thin wood specimens when the S1 and S3 layers have been severed (Plaza et al. 2016). Significant effects of the microfibril angle in the S1 and S3 layers was, however, only seen at 80% and 95% RH and at water-saturation (Table 5). This indicates that the restraining effect primarily occurs at these higher moisture states. This could partly explain why species like ash, beech and oak had moisture contents higher than average at high moisture states (Fig. 3), since these wood species were found to have a low microfibril angle in the S1 and S3 layers (Fig. 2b). The importance of this microfibril angle in explaining the variation in cell wall moisture content was highest at 95% RH and water-saturation (Table S8).

Considering the full moisture range, the cellulose crystallinity and hydroxyl accessibility were found to be only minor predictors of the cell wall moisture content (Table 5). The importance of these two characteristics was highest in the 20–80% RH-range (Table S8), and above this range, the importance decreased, and the hydroxyl accessibility was found not to be statistically significant at water-saturation (Table 5). For cellulose crystallinity, the correlation with the cell wall moisture content was found to be positive (Table S7), i.e., a higher cellulose crystallinity was associated with a higher cell wall moisture content. This was different from what is seen in literature data for ex-situ cellulose of various origins and treatments, where the crystallinity is negatively correlated with the moisture content at a given environment (Fig. S4). As for cellulose crystallinity, the hydroxyl accessibility was only a minor predictor for the cell wall moisture content in the statistical model (Table 5), and the correlation was counterintuitive since the moisture content was negatively correlated with hydroxyl accessibility (Table S7). That is, a higher hydroxyl accessibility was associated with a lower cell wall moisture content. In some other studies, a higher hydroxyl accessibility resulted in a higher moisture content (Popescu et al. 2014; Rautkari et al. 2013), but

these studies were performed on wood chemically altered by thermal (Rautkari et al. 2013) or chemical (Popescu et al. 2014) modification to achieve different hydroxyl accessibilities. However, such modifications change various material characteristics other than the hydroxyl accessibility. Additionally, Rautkari et al. (2013) questioned the importance of the hydroxyl accessibility in controlling the cell wall moisture content, and Thybring et al. (2020b) showed that the internal space within cell walls after chemical modification were correlated with the cell wall moisture content, but not the hydroxyl accessibility. In the present study, we used untreated wood only and hereby avoided chemical and physical effects of modification. However, the wood species differed across physical properties (Fig. 2), therefore we cannot dismiss that the counterintuitive relation between hydroxyl accessibility and moisture content is an effect of a correlation between crystallinity and hydroxyl accessibility of cellulose (Fig. S5). A very minor predictor of the cell wall moisture content in the 20–80% RH-range was the bulk density, showing a slightly positive correlation (Table S7). The partial  $R^2$ -value (Table S8) was, however, considerably lower than any of the other statistically significant characteristics.

As described above, the difference in moisture content between wood species was higher at 95% RH and at water-saturation than at lower humidity levels (Fig. 3). In addition, for several wood characteristics (e.g. microfibril angle, chemical composition) different results were obtained when including or excluding the two highest moisture levels. It is therefore possible that some wood characteristics are more important for the equilibrium moisture content at low humidity levels and some are more important at higher humidity levels. This points to a difference in material behaviour in the 0–80% RH range compared to very humid conditions or at water-saturation. One material related difference between the low and high moisture ranges is the mobility of the hemicelluloses. These undergo softening (glass transition) that significantly decreases their stiffness when the wood moisture content reaches around 10–16% at room temperature (Jakes et al. 2019). Speculative, this change within the material might be a contributing factor to the shift in which wood characteristics that are most decisive for the equilibrium moisture content.

The statistically guided data exploration using backward elimination was not intended to reveal the fundamental mechanisms governing moisture sorption in wood cell walls. However, the analysis identified several wood characteristics that appear to correlate with the cell wall moisture content as well as a shift in behaviour between the high and low humidity states. Particularly noteworthy was the influence of the microfibril angle in the S1 and S3 layers on the cell wall moisture content, which warrants further investigations.

## Conclusion

Several wood characteristics were identified to be statistically significantly correlated with the cell wall moisture content. While the chemical composition was found to be a predictor of the cell wall moisture content at all moisture conditions, the influence of other wood characteristics differed between the low moisture range and the humid and saturated conditions. One of these was the microfibril angle in the S1 and S3 layers, which was identified as a more important characteristic at humid and saturated conditions than at lower humidity levels.

**Acknowledgments** The authors gratefully acknowledge Monica Fongen at the Norwegian Institute of Bioeconomy Research for her work performing TG/DSC/FTIR analysis. The late Bengt Nilsson at Lund University is also gratefully acknowledged for performing sorption balance measurements.

**Author contributions** Conceptualization: EE Thybring, M Fredriksson; Methodology: EE Thybring, M Fredriksson, T Nord-Larsen; Investigation: M Fredriksson, EE Thybring, M Rüggeberg, G Beck; Formal analysis: T Nord-Larsen, EE Thybring, M Rüggeberg, G Beck; Writing—original draft preparation: EE Thybring, M Fredriksson; Writing—review and editing: M Fredriksson, EE Thybring, M Rüggeberg, T Nord-Larsen, G Beck; Visualization: EE Thybring; Funding acquisition: M Fredriksson, EE Thybring; Project administration: EE Thybring, M Fredriksson.

**Funding** Open access funding provided by Lund University. Funding was provided by the Swedish Research Council FORMAS grant numbers: 2018–00387 and 2017–00871, the VILLUM Foundation postdoc programme, and Interreg Öresund-Kattegat-Skagerrak.

**Data availability** Data are available in the supplemental material provided with this article.

## Declarations

**Conflicts of interest** The authors have no relevant financial or non-financial interests to disclose.

**Open Access** This article is licensed under a Creative Commons Attribution 4.0 International License, which permits use, sharing, adaptation, distribution and reproduction in any medium or format, as long as you give appropriate credit to the original author(s) and the source, provide a link to the Creative Commons licence, and indicate if changes were made. The images or other third party material in this article are included in the article's Creative Commons licence, unless indicated otherwise in a credit line to the material. If material is not included in the article's Creative Commons licence and your intended use is not permitted by statutory regulation or exceeds the permitted use, you will need to obtain permission directly from the copyright holder. To view a copy of this licence, visit <http://creativecommons.org/licenses/by/4.0/>.

## References

- Ahlgren PA, Wood JR, Goring DAI (1972) Fiber saturation point of various morphological subdivisions of Douglas-fir and aspen wood. *Wood Sci Technol* 6:81–84
- Ahmet K, Dai G, Tomlin R, Kaczmar P, Riddiough S (2000) The equilibrium moisture content of common U.K. Species at three conditions of temperature and relative humidity. *For Prod J* 50:64
- Arzola-Villegas X, Lakes R, Plaza NZ, Jakes JE (2019) Wood moisture-induced swelling at the cellular scale—ab intra. *Forests* 10:996
- Atalla RH, Brady JW, Matthews JF, Ding S-Y, Himmel ME (2009) Structures of plant cell wall celluloses. In: Himmel ME (ed) *Biomass recalcitrance - deconstructing the Plant Cell Wall for Bioenergy*, 1 edn. Blackwell Publishing Ltd., Oxford, UK, pp 188–212
- Balashov V, Preston RD, Ripley GW, Spark LC (1957) Structure and mechanical properties of vegetable fibres. I. the influence of strain on the orientation of cellulose microfibrils in sisal leaf fibre. *Proc Royal Soc London Ser B-Biol Sci* 146:460–468
- Bergander A, Salmén L (2000) Variations in transverse fibre wall properties: relations between elastic properties and structure. *Holzforschung* 54:654–660
- Bergander A, Salmén L (2002) Cell wall properties and their effects on the mechanical properties of fibers. *J Mater Sci* 37:151–156
- Chen M, Zhang C, Shomali A, Coasne B, Carmeliet J, Derome D (2019) Wood–moisture relationships studied with molecular simulations: methodological guidelines. *Forests* 10:628
- Choong ET, Manwiller FG (1976) Dimensional and relative hygroscopic properties of hardwoods from Southern pine sites. *Wood Sci* 9:39–43
- Chow SZ (1972) Hydroxyl accessibility, moisture-content, and biochemical activity in cell-walls of Douglas-fir trees. *Tappi* 55:539–544

- Christensen GN, Kelsey KE (1958) Sorption of water vapour by constituents of wood: determination of sorption isotherms. *Aust J Appl Sci* 9:265–282
- Christensen GN, Kelsey KE (1959) Die Sorption von Wasserdampf durch die chemischen Bestandteile des Holzes (the sorption of water vapor by the constituents of wood). *Holz als Roh- und Werkstoff* 17:189–203. <https://doi.org/10.1007/BF02608811>
- Derome D, Griffa M, Koebel M, Carmeliet J (2011) Hysteretic swelling of wood at cellular scale probed by phase-contrast X-ray tomography. *J Struct Biol* 173:180–190
- Dworzanski J, Buchanan RM, Chapman JN, Meuzelaar HLC (1991) Characterization of lignocellulosic materials and model compounds by combined TG/(GC)/FTIR/MS. Paper presented at the 201st American Chemical Society National Meeting, Atlanta, GA, USA
- Elder T, Houtman C (2013) Time-domain NMR study of the drying of hemicellulose extracted aspen (*Populus tremuloides* Michx.). *Holzforschung* 67:405–411. <https://doi.org/10.1515/hf-2012-0130>
- Engelund ET, Thygesen LG, Hoffmeyer P (2010) Water sorption in wood and modified wood at high values of relative humidity. Part 2: Appendix. Theoretical assessment of the amount of capillary water in wood microvoids. *Holzforschung* 64:325–330. <https://doi.org/10.1515/hf.2010.061>
- Engelund ET, Thygesen LG, Svensson S, Hill CAS (2013) A critical discussion of the physics of wood-water interactions. *Wood Sci Technol* 47:141–161
- Feist WC, Tarkow H (1967) A new procedure for measuring fiber saturation points. *For Prod J* 17:65–68
- Fernandes AN et al (2011) Nanostructure of cellulose microfibrils in spruce wood. *Proc Natl Acad Sci USA* 108:E1195–E1203
- Fredriksson M (2019) On wood–water interactions in the over-hygroscopic moisture range—mechanisms, methods, and influence of wood modification. *Forests* 10:779
- Fredriksson M, Thybring EE (2019) On sorption hysteresis in wood: separating hysteresis in cell wall water and capillary water in the full moisture range. *PLoS ONE* 14:e0225111. <https://doi.org/10.1371/journal.pone.0225111>
- Füchtner S, Brock-Nannestad T, Smeds A, Fredriksson M, Pilgård A, Thygesen LG (2020) Hydrophobic and hydrophilic extractives in Norway Spruce and Kurile Larch and their role in Brown-Rot degradation. *Front Plant Sci* 11:885. <https://doi.org/10.3389/fpls.2020.00855>
- Gao X, Zhuang S, Jin J, Cao P (2015) Bound water content and pore size distribution in swollen cell walls determined by NMR technology. *Bioresour* 10(4):8208–8224
- Glass SV, Boardman CR, Zelinka SL (2017) Short hold times in dynamic vapor sorption measurements mischaracterize the equilibrium moisture content of wood. *Wood Sci Technol* 51:243–260. <https://doi.org/10.1007/s00226-016-0883-4>
- Glass SV, Boardman CR, Thybring EE, Zelinka SL (2018) Quantifying and reducing errors in equilibrium moisture content measurements with dynamic vapor sorption (DVS) experiments. *Wood Sci Technol* 52:909–927. <https://doi.org/10.1007/s00226-018-1007-0>
- Grønli MG, Várhegyi G, Di Blasi C (2002) Thermogravimetric analysis and devolatilization kinetics of Wood. *Ind Eng Chem Res* 41:4201–4208. <https://doi.org/10.1021/ie0201157>
- Harris JM, Meylan BA (1965) The influence of microfibril angle on longitudinal and tangential shrinkage in *Pinus radiata*. *Holzforschung* 19:144. <https://doi.org/10.1515/hfsg.1965.19.5.144>
- Hernández RE, Cáceres CB (2010) Magnetic resonance microimaging of liquid water distribution in sugar maple wood below fiber saturation point. *Wood Fiber Sci* 42:259–272
- Hill C, Altgen M, Rautkari L (2021) Thermal modification of wood—a review: chemical changes and hygroscopicity. *J Mater Sci* <https://doi.org/10.1007/s10853-020-05722-z>
- Hoffmeyer P, Engelund ET, Thygesen LG (2011) Equilibrium moisture content (EMC) in Norway spruce during the first and second desorptions. *Holzforschung* 65:875–882. <https://doi.org/10.1515/HF.2011.112>
- Hofstetter K, Hinterstoisser B, Salmén L (2006) Moisture uptake in native cellulose - the roles of different hydrogen bonds: a dynamic FT-IR study using deuterium exchange. *Cellulose* 13:131–145
- Howson JA (1949) Water sorption and the poly-phase structure of cellulose fibers. *Text Res J* 19:152–163. <https://doi.org/10.1177/004051754901900303>
- Jakes JE, Hunt CG, Zelinka SL, Ciesielski PN, Plaza NZ (2019) Effects of moisture on diffusion in unmodified wood cell walls: a phenomenological polymer science approach. *Forests* 10:1084
- Keylwerth R (1962) Untersuchungen über freie und behinderte Quellung von Holz—Erste Mitteilung: freie Quellung. *Holz als Roh- und Werkstoff* 20:252–259. <https://doi.org/10.1007/BF02604681>
- Lang ARG, Mason SG (1960) Tritium exchange between cellulose and water - accessibility measurements and effects of cyclic drying. *Can J Chemistry-Revue Canadienne De Chim* 38:373–387. <https://doi.org/10.1139/v60-053>
- Lindh EL, Bergensträhle-Wohlert M, Terenzi C, Salmén L, Furó I (2016) Non-exchanging hydroxyl groups on the surface of cellulose fibrils: the role of interaction with water. *Carbohydr Res* 434:136–142. <https://doi.org/10.1016/j.carres.2016.09.006>
- Loelovitch M, Gordeev M (1994) Crystallinity of cellulose and its accessibility during deuteration. *Acta Polym* 45:121–123. <https://doi.org/10.1002/actp.1994.010450211>
- Mann J, Marrinan HJ (1956) The reaction between cellulose and heavy water. 2.-measurement of absolute accessibility and crystallinity. *Trans Faraday Soc* 52:487–492. <https://doi.org/10.1039/tf9565200487>
- Meylan BA (1972) Influence of microfibril angle on longitudinal shrinkage-moisture content relationship. *Wood Sci Technol* 6:293–301
- Murata K, Masuda M (2006) Microscopic observation of transverse swelling of latewood tracheid: effect



- of macroscopic/mesoscopic structure. *J Wood Sci* 52:283–289
- Newlin JA, Wilson TRC (1919) The relation of the shrinkage and strength properties of wood to its specific gravity, vol 676. US department of agriculture, Washington DC, USA
- Noack D, Schwab E, Bartz A (1973) Characteristics for a judgment of sorption and swelling behavior of wood. *Wood Sci Technol* 7:218–236
- Nopens M, Wadsö L, Ortmann C, Fröba M, Krause A (2019) Measuring the heat of interaction between lignocellulosic materials and water. *Forests* 10:674
- Nzokou P, Kamden DP (2004) Influence of wood extractives on moisture sorption and wettability of red oak (*Quercus rubra*), black cherry (*Prunus serotina*), and red pine (*Pinus resinosa*). *Wood Fiber Sci* 36:483–492
- O'Sullivan AC (1997) Cellulose: the structure slowly unravels. *Cellulose* 4:173–207
- Passarini L, Malveau C, Hernández R (2015) Distribution of the equilibrium moisture content in four hardwoods below fiber saturation point with magnetic resonance microimaging. *Wood Sci Technol* 49:1251–1268. <https://doi.org/10.1007/s00226-015-0751-7>
- Patera A, Derome D, Griffa M, Carmeliet J (2013) Hysteresis in swelling and in sorption of wood tissue. *J Struct Biol* 182:226–234. <https://doi.org/10.1016/j.jsb.2013.03.003>
- Patera A, Van den Bulcke J, Boone MN, Derome D, Carmeliet J (2018) Swelling interactions of earlywood and latewood across a growth ring: global and local deformations. *Wood Sci Technol* 52:91–114. <https://doi.org/10.1007/s00226-017-0960-3>
- Pennings AJ, Prins W, Hale RD, Rånby BG (1961) Inter- and intramolecular order in regenerated cellulose. *J Appl Polym Sci* 5:676–684
- Plaza NZ (2019) On the experimental assessment of the molecular-scale interactions between wood and water. *Forests* 10:616
- Plaza NZ, Pingali SV, Qian S, Heller WT, Jakes JE (2016) Informing the improvement of forest products durability using small angle neutron scattering. *Cellulose* 23:1593–1607. <https://doi.org/10.1007/s10570-016-0933-y>
- Pönni R, Rautkari L, Hill CAS, Vuorinen T (2014) Accessibility of hydroxyl groups in birch kraft pulps quantified by deuterium exchange in D<sub>2</sub>O vapor. *Cellulose* 21:1217–1226. <https://doi.org/10.1007/s10570-014-0166-x>
- Popescu C-M, Hill CAS, Curling S, Ormondroyd G, Xie Y (2014) The water vapour sorption behaviour of acetylated birch wood: how acetylation affects the sorption isotherm and accessible hydroxyl content. *J Mater Sci* 49:2362–2371. <https://doi.org/10.1007/s10853-013-7937-x>
- Rafsanjani A, Stiefel M, Jefimovs K, Mokso R, Derome D, Carmeliet J (2014) Hygroscopic swelling and shrinkage of latewood cell wall micropillars reveal ultrastructural anisotropy. *J Royal Soc Interface* 11(95):20140126. <https://doi.org/10.1098/rsif.2014.0126>
- Rautkari L, Hill CAS, Curling S, Jalaludin Z, Ormondroyd G (2013) What is the role of the accessibility of wood hydroxyl groups in controlling moisture content? *J Mater Sci* 48:6352–6356. <https://doi.org/10.1007/s10853-013-7434-2>
- Ringman R, Beck G, Pilgård A (2019) The importance of moisture for brown rot degradation of modified wood: a critical discussion. *Forests* 10:522
- Rüggeberg M, Saxe F, Metzger TH, Sundberg B, Fratzl P, Burgert I (2013) Enhanced cellulose orientation analysis in complex model plant tissues. *J Struct Biol* 183:419–428. <https://doi.org/10.1016/j.jsb.2013.07.001>
- Salmén L, Bergström E (2009) Cellulose structural arrangement in relation to spectral changes in tensile loading FTIR. *Cellulose* 16:975–982
- Skaar C (1984) Wood water relationships, vol series. *Adv Chem*, 127–172
- Simpson LA, Barton AFM (1991) Determination of the fibre saturation point in whole wood using differential scanning calorimetry. *Wood Sci Technol* 25:301–308. <https://doi.org/10.1007/BF00225469>
- Taniguchi T, Harada H, Nakato K (1978) Determination of water-adsorption sites in wood by a hydrogen-deuterium exchange. *Nature* 272:230–231
- Thybring EE, Fredriksson M, Zelinka SL, Glass SV (2022) Water in wood: a review of current understanding and knowledge gaps. *Forests* 13:2051. <https://doi.org/10.3390/f13122051>
- Thygesen LG, Englund ET, Hoffmeyer P (2010) Water sorption in wood and modified wood at high values of relative humidity. Part I: Results for untreated, acetylated, and furfurylated Norway spruce. *Holzforschung* 64:315–315. <https://doi.org/10.1515/hf.2010.044>
- Thybring EE, Thygesen LG, Burgert I (2017) Hydroxyl accessibility in wood cell walls as affected by drying and re-wetting procedures. *Cellulose* 24:2375–2384. <https://doi.org/10.1007/s10570-017-1278-x>
- Thybring EE, Glass SV, Zelinka SL (2019) Kinetics of water vapor sorption in wood cell walls: state of the art and research needs. *Forests* 10:704
- Thybring EE, Digaitis R, Nord-Larsen T, Beck G, Fredriksson M (2020a) How much water can wood cell walls hold? A triangulation approach to determine the maximum cell wall moisture content. *PLoS ONE* 15:e0238319. <https://doi.org/10.1371/journal.pone.0238319>
- Thybring EE, Piqueras S, Tarmian A, Burgert I (2020b) Water accessibility to hydroxyls confined in solid wood cell walls. *Cellulose* 27:5617–5627. <https://doi.org/10.1007/s10570-020-03182-x>
- Vahtikari K, Rautkari L, Noponen T, Lillqvist K, Hughes M (2017) The influence of extractives on the sorption characteristics of Scots pine (*Pinus sylvestris* L.). *J Mater Sci* 52:10840–10852. <https://doi.org/10.1007/s10853-017-1278-0>
- Venkateswaran A (1970) Sorption of aqueous and nonaqueous media by wood and cellulose. *Chem Rev* 70:619–637
- Verlhac C, Dedier J, Chanzy H (1990) Availability of surface hydroxyl-groups in Valonia and bacterial cellulose. *J Polym Sci Part A-Polymer Chem* 28:1171–1177
- Vorreiter L (1963) Fasersättigungsfeuchte und höchste Wasseraufnahme der Hölzer in memoriam Wilhelm Klauwitz. *Holzforschung* 17:139. <https://doi.org/10.1515/hfsg.1963.17.5.139>

- Wang N, Liu W, Peng Y (2013) Gradual transition zone between cell wall layers and its influence on wood elastic modulus. *J Mater Sci* 48:5071–5084. <https://doi.org/10.1007/s10853-013-7295-8>
- Wangaard FF, Granados LA (1967) The effect of extractives on water-vapor sorption by wood. *Wood Sci Technol* 1:253–277
- Williams DR (1995) The characterisation of powders by gravimetric water vapour sorption. *Int LABMATE* 20:40–42
- Yamashita K, Hirakawa Y, Nakatani H, Ikeda M (2009) Tangential and radial shrinkage variation within trees in sugi (*Cryptomeria japonica*) cultivars. *J Wood Sci* 55:161–168. <https://doi.org/10.1007/s10086-008-1012-2>
- Yang H, Yan R, Chen H, Lee DH, Zheng C (2007) Characteristics of hemicellulose, cellulose and lignin pyrolysis. *Fuel* 86:1781–1788. <https://doi.org/10.1016/j.fuel.2006.12.013>
- Yang T, Ma E, Cao J (2018) Effects of lignin in wood on moisture sorption and hygroexpansion tested under dynamic conditions. *Holzforschung* 72:943. <https://doi.org/10.1515/hf-2017-0198>
- Yang T, Thybring EE, Fredriksson M, Ma E, Cao J, Digaitis R, Thygesen LG (2020) Effects of changes in biopolymer composition on moisture in acetylated wood. *Forests* 11:719
- Zabler S, Paris O, Burgert I, Fratzl P (2010) Moisture changes in the plant cell wall force cellulose crystallites to deform. *J Struct Biol* 171:133–141
- Zelinka SL, Lambrecht MJ, Glass SV, Wiedenhoef AC, Yelle DJ (2012) Examination of water phase transitions in Loblolly pine and cell wall components by differential scanning calorimetry. *Thermochim Acta* 533:39–45. <https://doi.org/10.1016/j.tca.2012.01.015>
- Zhou H, Xu R, Ma E (2016) Effects of removal of chemical components on moisture adsorption by wood. *Bioresource* 11(2):3110–3122

**Publisher's Note** Springer Nature remains neutral with regard to jurisdictional claims in published maps and institutional affiliations.